12PFL-0413

Validation of a Thermal-Electric Li-Ion Battery Model

Author, co-author list (Do NOT enter this information. It will be pulled from participant tab in MyTechZone)

Affiliation (Do NOT enter this information. It will be pulled from participant tab in MyTechZone)

ABSTRACT

Commercial vehicle manufacturers are investing substantial resources into the development and testing of advanced battery systems for the next generation of hybrid and electric vehicles. Likewise the US army is investing in lithium ion battery research for power and energy applications including SLI (starter, lights, and ignition), silent watch, unmanned vehicles, and directed energy weapons. A major design constraint is the management of the heat generated by Li-Ion battery systems. Extreme battery temperatures impact both the performance and reliability of the battery system as well as the overall operation of the vehicle. Analysis tools that can address vehicle and battery thermal management issues are needed to accelerate this development. To meet that need, a coupled thermal-electric model for battery cells and packs has been developed and implemented into the existing thermal modeling software RadTherm. This paper documents the comparison of physical test results with a computer model of the thermal response for an actual vehicle Li-Ion battery cell.

The thermo-electrical battery model described in this paper predicts an effective driving potential and internal conductance for a cell based on the cell environmental temperature and measure of state of charge. From these parameters a local current density is computed and applied to an electrical model of the voltage distribution on the electrodes. Heat generation is derived from the local voltage difference across the electrodes and the current density between electrodes and then applied to a thermal model to predict local temperature rise over the cell.

When applied to a cell, the battery model is useful for predicting the effects of cell size, tab location, and current collector thickness on voltage distribution and local heat generation. The model can also be applied to a multi-cell pack to study the effects of various thermal management strategies. In either application, battery loads corresponding to pre-determined drive cycles can be applied to the model to evaluate the ability of a particular cell or pack design to supply vehicle power in a given operating scenario. In this paper we describe the implementation of the model, compare model predictions to electrical and thermal measurements taken on a test cell, demonstrate the effects of different cell configurations on voltage and temperature distributions, and the show the relative effectiveness of various cooling schemes (natural and forced air convection and edge cooling) applied to a pack.

INTRODUCTION

The automotive industry as well as the Army is in the process of developing alternative power and energy sources for vehicles and other military applications. There is a growing interest in electric or hybrid electric vehicles employing batteries to provide part or all of the energy needed for motive power. Because batteries generate heat when charged or discharged, and their performance parameters depend on their operating temperature, there is a need for robust thermal management systems dedicated to the battery. The design of these systems requires modeling tools capable of simulating the interaction of a battery with the power and thermal management subsystems in the vehicle.

Many OEMs and component suppliers use a general thermal analysis code called RadTherm[1] for thermal simulation and design assessment. A battery module has been added to RadTherm to facilitate modeling of the electrical and thermal behavior of a battery integrated with a thermal management system. In this paper, we describe the electro-thermal model and its implementation in RadTherm, compare the model output with validation data, and give examples of how the model can be employed in modeling studies to answer thermal management design issues.

REPORT DOCUMENTATION PAGE

Form Approved
OMB No. 0704-0188

1. REPORT DATE *(DD-MM-YYYY)*	2. REPORT TYPE	3. DATES COVERED *(From - To)*
07/11/2011	Journal Article	08/03/2011 to 12/10/2011

4. TITLE AND SUBTITLE
Validation of a Thermal-Electric Li-Ion Battery Model

5a. CONTRACT NUMBER

5b. GRANT NUMBER

5c. PROGRAM ELEMENT NUMBER

6. AUTHOR(S)
Scott D. Peck
Ted Olszanski
Sonya Zanardelli

5d. PROJECT NUMBER

5e. TASK NUMBER

5f. WORK UNIT NUMBER

7. PERFORMING ORGANIZATION NAME(S) AND ADDRESS(ES)
Thermo Analytics
23440 Airpark Boulevard
Calumet, MI 49913

8. PERFORMING ORGANIZATION REPORT NUMBER

9. SPONSORING/MONITORING AGENCY NAME(S) AND ADDRESS(ES)
TARDEC Technical Information Center
6501 E. 11 Mile Rd.
Warren, MI 48397-5000

10. SPONSOR/MONITOR'S ACRONYM(S)

11. SPONSORING/MONITORING AGENCY REPORT NUMBER
22431

12. DISTRIBUTION AVAILABILITY STATEMENT
Distribution A

13. SUPPLEMENTARY NOTES
For 2012 SAE International

14. ABSTRACT

Commercial vehicle manufacturers are investing substantial resources into the development and testing of advanced battery systems for the next generation of hybrid and electric vehicles. Likewise the US army is investing in lithium ion battery research for power and energy applications including SLI (starter, lights, and ignition), silent watch, unmanned vehicles, and directed energy weapons. A major design constraint is the management of the heat generated by Li-Ion battery systems. Extreme battery temperatures impact both the performance and reliability of the battery system as well as the overall operation of the vehicle. Analysis tools that can address vehicle and battery thermal management issues are needed to accelerate this development. To meet that need, a coupled thermalelectric model for battery cells and packs has been developed and implemented into the existing thermal modeling software RadTherm. This paper documents the comparison of physical test results with a computer model of the thermal response for an actual vehicle Li-Ion battery cell.

15. SUBJECT TERMS

16. SECURITY CLASSIFICATION OF:			17. LIMITATION OF ABSTRACT	18. NUMBER OF PAGES	19a. NAME OF RESPONSIBLE PERSON
a. REPORT	b. ABSTRACT	c. THIS PAGE	Public Release	17	Christopher Thurman
Unclass	Unclass	Unclass			19b. TELEPONE NUMBER (*Include area code*) 586.282.5377

INSTRUCTIONS FOR COMPLETING SF 298

1. REPORT DATE. Full publication date, including day, month, if available. Must cite at lest the year and be Year 2000 compliant, e.g., 30-06-1998; xx-08-1998; xx-xx-1998.

2. REPORT TYPE. State the type of report, such as final, technical, interim, memorandum, master's thesis, progress, quarterly, research, special, group study, etc.

3. DATES COVERED. Indicate the time during which the work was performed and the report was written, e.g., Jun 1997 - Jun 1998; 1-10 Jun 1996; May - Nov 1998; Nov 1998.

4. TITLE. Enter title and subtitle with volume number and part number, if applicable. On classified documents, enter the title classification in parentheses.

5a. CONTRACT NUMBER. Enter all contract numbers as they appear in the report, e.g. F33615-86-C-5169.

5b. GRANT NUMBER. Enter all grant numbers as they appear in the report, e.g. 1F665702D1257.

5c. PROGRAM ELEMENT NUMBER. Enter all program element numbers as they appear in the report, e.g. AFOSR-82-1234.

5d. PROJECT NUMBER. Enter al project numbers as they appear in the report, e.g. 1F665702D1257; ILIR.

5e. TASK NUMBER. Enter all task numbers as they appear in the report, e.g. 05; RF0330201; T4112.

5f. WORK UNIT NUMBER. Enter all work unit numbers as they appear in the report, e.g. 001; AFAPL30480105.

6. AUTHOR(S). Enter name(s) of person(s) responsible for writing the report, performing the research, or credited with the content of the report. The form of entry is the last name, first name, middle initial, and additional qualifiers separated by commas, e.g. Smith, Richard, Jr.

7. PERFORMING ORGANIZATION NAME(S) AND ADDRESS(ES). Self-explanatory.

8. PERFORMING ORGANIZATION REPORT NUMBER. Enter all unique alphanumeric report numbers assigned by the performing organization, e.g. BRL-1234; AFWL-TR-85-4017-Vol-21-PT-2.

9. SPONSORING/MONITORS AGENCY NAME(S) AND ADDRESS(ES). Enter the name and address of the organization(s) financially responsible for and monitoring the work.

10. SPONSOR/MONITOR'S ACRONYM(S). Enter, if available, e.g. BRL, ARDEC, NADC.

11. SPONSOR/MONITOR'S REPORT NUMBER(S). Enter report number as assigned by the sponsoring/ monitoring agency, if available, e.g. BRL-TR-829; -215.

12. DISTRIBUTION/AVAILABILITY STATEMENT. Use agency-mandated availability statements to indicate the public availability or distribution limitations of the report. If additional limitations/restrictions or special markings are indicated, follow agency authorization procedures, e.g. RD/FRD, PROPIN, ITAR, etc. Include copyright information.

13. SUPPLEMENTARY NOTES. Enter information not included elsewhere such as: prepared in cooperation with; translation of; report supersedes; old edition number, etc.

14. ABSTRACT. A brief (approximately 200 words) factual summary of the most significant information.

15. SUBJECT TERMS. Key words or phrases identifying major concepts in the report.

16. SECURITY CLASSIFICATION. Enter security classification in accordance with security classification regulations, e.g. U, C, S, etc. If this form contains classified information, stamp classification level on the top and bottom of this page.

17. LIMITATION OF ABSTRACT. This block must be completed to assign a distribution limitation to the abstract. Enter UU (Unclassified Unlimited) or SAR (Same as Report). An entry in this block is necessary if the abstract is to be limited.

BATTERY MODEL

The electro-thermal model chosen to describe battery behavior is an empirical approach that seeks to describe the current-voltage relationship of a battery with fitting parameters that are functions of the depth-of-discharge of a cell, and the temperature of the cell. The fitting parameters are an *effective* open cell voltage, and an *effective* internal conductance of the cell. The model has been described in the literature[2,3,4]. It relates the current density passing from cathode to anode to the voltage difference from cathode to anode, thus:

$$J = Y[V_p - V_n - U] \qquad (1)$$

where J is the current density, V_p the voltage on the cathode, V_n the voltage on the anode, Y is the fitting parameter representing the internal conductance of the cell, and U is the fitting parameter representing an effective open cell voltage. Note that in this formulation, a cell discharge corresponds to a negative current density.

The fitting parameters are functions of the depth of discharge and ambient temperature, thus

$$U = \sum_i \sum_j \alpha_{ij} T^j DoD^i \qquad (2)$$

and

$$Y = \sum_i \sum_j \beta_{ij} T^j DoD^i \qquad (3)$$

where the α_{ij} and β_{ij} are the coefficients of a polynomial curve fit of the U and Y parameters, T is the ambient or environmental temperature at which the discharge measurements were made, and DoD is the depth of discharge, defined as

$$DoD = \frac{A\int Jdt}{Capacity} \qquad (4)$$

A is the area of the cell, t is time in hours, and capacity is the rated capacity of the cell in ampere-hours.

The current is distributed to the electrodes via metallic collector plates. These collector plates have a voltage distribution on them that is described by Poisson's equation (see Figure 1). On the collector plate for the anode,

$$\nabla^2 V_n = \frac{J}{\sigma_n t_n} \qquad (5)$$

where σ_n is the electrical conductivity and t_n is the total thickness of the anode collector plate.

On the cathode collector plate,

$$\nabla^2 V_p = -\frac{J}{\sigma_p t_p} \qquad (6)$$

where σ_p is the electrical conductivity and t_p is the total thickness of the cathode collector plate.

The heat generation due to current transfer from cathode to anode, $\dot{q}_e'''$ is described by

$$\dot{q}'''_e = \frac{J}{t}\left[V_p - V_n - E_{oc} + T\frac{dE_{oc}}{dT} \right] \qquad (7)$$

Here t is the total thickness of the cell and E_{oc} is the open cell voltage.

The product of the current and the sum of the first three terms in the brackets is the irreversible heating due to cell polarization, and is always positive (given the convention of discharge equates to negative current). The last term in brackets represents the reversible heat due to the entropy of reaction, and is positive (exothermic) for cell charging, and negative (endothermic) during cell discharge[5,6].

There is resistive heating in the collector plates, described by

$$\dot{q}'''_c = -J_c \cdot \nabla V_c = \sigma_c (\nabla V_c \cdot \nabla V_c) \qquad (8)$$

Here the subscript c refers to either the anode collector (n) or the cathode collector (p).

We assume the temperature through the thickness of the cell is uniform, and is described in the other two dimensions by

$$\rho C \frac{\partial T}{\partial t} = k\nabla^2 T + \dot{q}''' - 2h(T - T_a)/t \qquad (9)$$

Here, $\dot{q}''' = \dot{q}'''_e + \dot{q}'''_n + \dot{q}'''_p$, ρ is the average density of the cell, C the average specific heat of the cell materials, k the average or effective thermal conductivity of the cell materials, h is the effective heat transfer coefficient between the cell surface and the ambient environment, and T_a is the effective ambient temperature. In this formulation, convection and radiation have been combined into the effective h and T_a.

IMPLEMENTATION

We have developed a methodology to solve the combined thermo-electric problem formulated in the preceding section using RadTherm. The approach is to use two meshes, one representing the two collector plates on which the voltage distribution is calculated, and a separate mesh representing the thermal behavior of the electrode/collector plate sandwich comprising a single cell. We employ a thermal analog to solve the electrical problem, wherein the ‘temperature’ output in the electrical part of the model is interpreted as voltage, and the ‘heat flow’ is interpreted as current. The electrical problem is illustrated conceptually in Figure 1, and the thermal problem is shown conceptually in Figure 2.

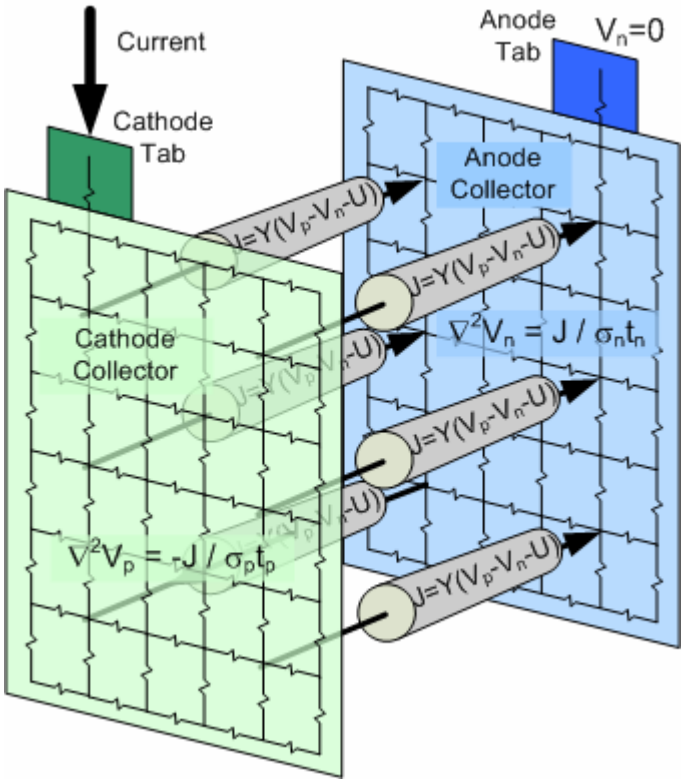

Figure 1. A conceptual representation of the electrical part of the model implemented in RadTherm.

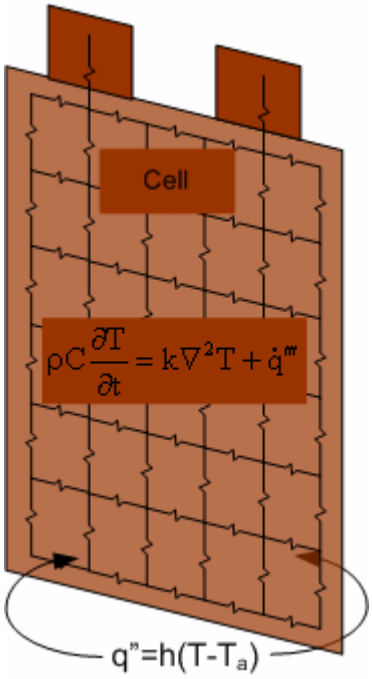

Figure 2. A conceptual representation of the thermal part of the model implemented in RadTherm.

In the electrical problem the voltage is constrained to be zero on the anode tab, and a net current is imposed on the cathode tab. A set of custom functions implemented as a plug-in module to RadTherm is employed to impose the proper local value of current density at each anode and cathode node. The current density is computed using equation (1), using the local nodal values of V_p and V_n obtained from the electrical solution.

Simultaneously, the nodal values of V_p and V_n are used to compute the local heating value from equations (7) and (8). This heat is imposed by the plug-in module on the appropriate nodes in the thermal part of the model. The thermal model also includes conventional thermal boundary conditions on the cell, i.e., convection and radiation from the face of the cell, with the possibility of adding conduction through the cell edges to cooled plates or fins.

The thermal model is transient. The electrical model is steady-state in the sense that there is no 'capacitance' in the electrical mesh, but transient current boundary conditions can be imposed on the model. The cell behavior also changes in response to the time-dependent computation of the local value of depth of discharge on the cell electrodes. During the solution, the plug-in module also adjusts the fitting parameters U and Y in response to changes in the ambient temperature being applied to the cell.

VALIDATION

Measurements on a lithium-ion cell were made to provide data for validation of the model. Terminal voltage and cell surface temperature were measured during constant current discharges in a controlled environment. The cell was simulated in the RadTherm software using the model described above, and the output of the model is compared to the measurements below.

TEST SETUP

A pouch type cell from A123 Systems was used for the test measurements and subsequent validation model. The cell stores 19.6 A-hr (63.3 W-hr). It was chosen because it is suitable as the basic building block for the large battery packs foreseen for commercial and military vehicle applications. The cell is approximately 6.35 mm thick, 160 mm in width, and 230 mm in height and weighs approximately 0.5 kg. The manufacturer's literature states the specific energy is 132 W-h/kg with an energy density of 282 W-h/L.

The test procedure calls for characterizing the cell at constant discharge rates of 0.5C, 1C, 3C, and 5C at 25 ^{o}C, 0 ^{o}C, and 45 ^{o}C utilizing a Bitrode MCV16-60-6 cell cycler unit. Three circuits were operated in parallel to attain sufficient current capacity to discharge at the high rate. Additionally, five (5) thermocouple sensors recorded thermal readings across the face of the cell and a control thermocouple provided an over temperature safety control. See Figure 3. An explosion proof Tenney T10RC-1.5 environmental chamber shown in Figure 4 thermally controlled the cell test articles during performance testing. The thermocouple sensors were augmented by a FLIR SC620 portable programmable infrared camera which was suspended within the chamber directly over the test article and recorded thermal images at discharge rate dependent intervals. A flat black paint was applied across the surface of the cell to increase emissivity and improve the camera's ability to measure subtle surface temperature differences. The cell was placed flat on a fiberglass tray so only one side was convectively cooled. The test setup is shown in Figure 5.

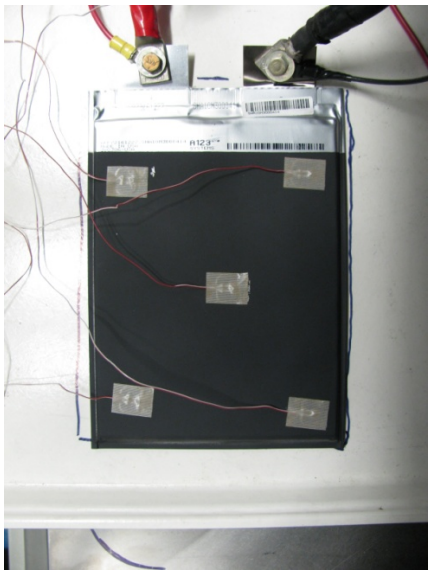

Figure 3. A123 cell with thermocouples.

Figure 4. Tenney Environmental Chamber.

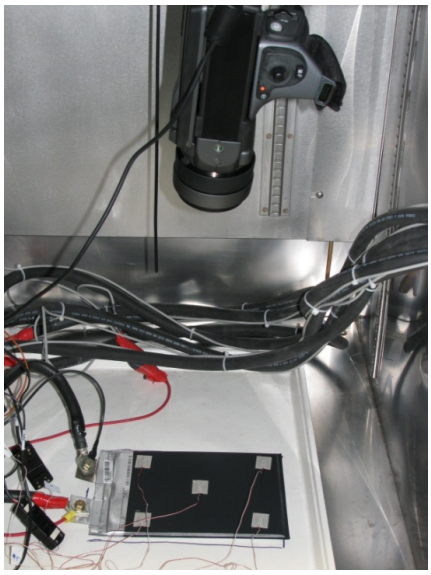

Figure 5. Test Setup.

TARDEC Energy Storage Team/Labs:

The Mission of the U.S. Army Tank Automotive Research, Development and engineering Center (TARDEC) Ground Vehicle Power and Mobility Energy Storage Team is to 1) pursue energy storage technology, development, component test and evaluation, 2) identify technology barriers and develop technical solutions, 3) provide technical support to customers, other teams and government agencies for all energy storage requirements, and 4) provide cradle to grave support for all Army energy storage systems. Application areas include rechargeable high energy/high power batteries, ultra capacitors, standard military SLI lead acid batteries, hybrid power sources, Silent Watch, and energy storage for directed energy weapons.

TARDEC's current cell and battery testing capability is spread over two distinct laboratory areas. The first is the **Lead Acid Battery Laboratory (Bldg 7)** which supports testing and pre-qualification of military lead acid batteries. The lab contains 6 water baths, 31 battery circuits, 48 single cell circuits, and 2 thermal chambers. The second is the **Electrochemical Research & Analysis Lab**

(EARL) which supports small scale testing for advanced battery chemistries (Li-ion, Ni-Zn) at the cell, module level, and for battery R&D projects. The lab has a walk-in fume hood for safety, 2 explosion resistant thermal chambers, and 20 cell and battery circuits.

Future capabilities will expand with the completion of the **Ground Systems Power and Energy Laboratories (GSPEL).** The Lead Acid Battery Laboratory will move into the new GSPEL building and join the three interior cell/battery test rooms and three exterior pack test chambers designed for safe testing. The GSPEL will also add a Battery Management System (BMS) Electronics Lab that allows TRL level BMS evaluation along with hardware-in-loop simulations and cell/battery storage and shelf life testing facilities.

CELL MODEL

A RadTherm model of the test cell was created to simulate the test results. The model is shown in Figure 6. In the electrical part of the model, the cathode collector and tab is aluminum and the anode collector and tab is copper. In the thermal model, the cell is modeled as four layers, one layer each for the cathode, cathode collector, anode, and anode collector, respectively. This is done to simplify the assignment of thermal properties.

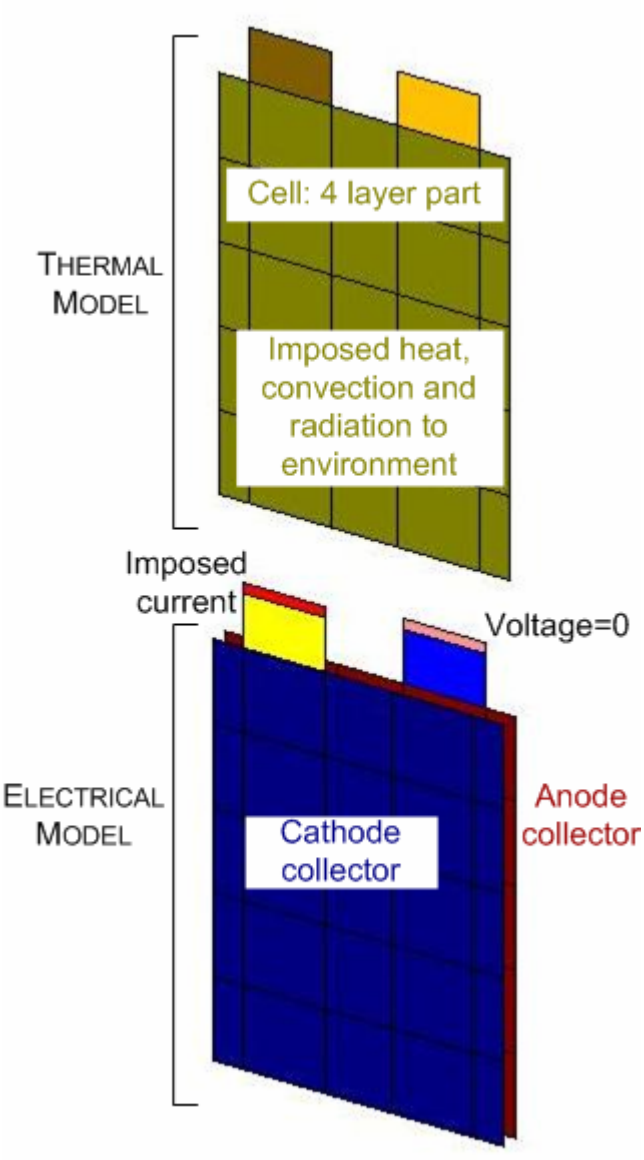

Figure 6. The RadTherm battery model consists of an electrical part and a thermal part.

The voltage of the anode tab is set to zero, and the discharge current is imposed on the cathode tab. A steady-state solution of the voltage distribution on the collectors at the specified initial discharge current is found, from which the heating terms are derived and used for the initial time step starting condition.

In the thermal model, the initial temperature of the entire cell is set to the environmental temperature for the particular test being simulated. The convection coefficient on the exposed side of the cell is computed by library convection functions in RadTherm. For the conditions of the test, typical values of the heat transfer coefficient were in the range of 3 to 8 W/m^2-C. The fluid temperature is set to the environmental temperature. The side of the cell lying on the test chamber surface is assumed to be insulated. The emissivity of the exposed surface is set to a value of 0.95 (the cell was painted black to facilitate capturing thermal imagery of the discharge transient). Heating in the cables connecting the cell to the power supply was assumed to be negligible due to the size of the conductors. The initial condition for the thermal model was the environmental temperature.

RESULTS

Figures 7 to 9 show a comparison of the measured terminal voltage obtained at different discharge rates with the value predicted by RadTherm using the correlation described above. Figure 7 is at an environmental temperature of 5 °C, and shows good agreement between data and RadTherm (curve fit) at 1C and 3C. Agreement at the extremes of the discharge rates is not as good. This is attributed to curvature of the voltage versus current density curves shown in Figure 10. The battery model assumes linear behavior, and therefore the curve fit would be expected to provide good results near the points of intersection of a line and the curve, as is the case. At higher temperatures, (Figures 8 and 9), the agreement is better, because the voltage versus current density behavior is closer to the linear assumption, as shown in Figure 11.

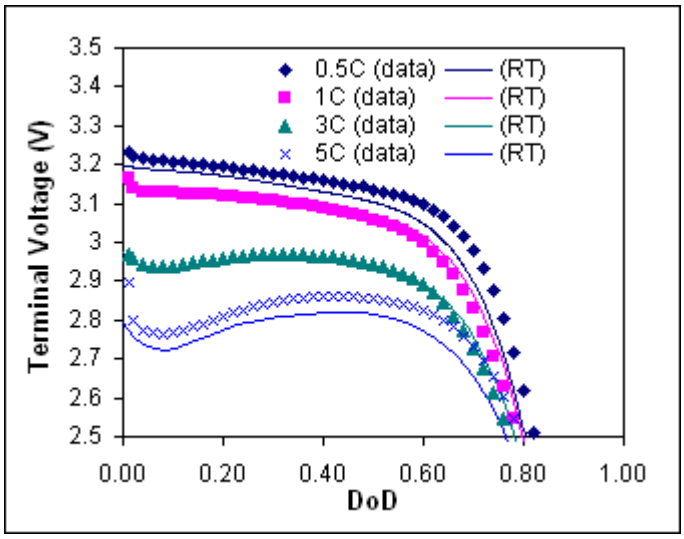

Figure 7. Terminal voltage predicted by RadTherm compared to measurements taken at 5 ºC.

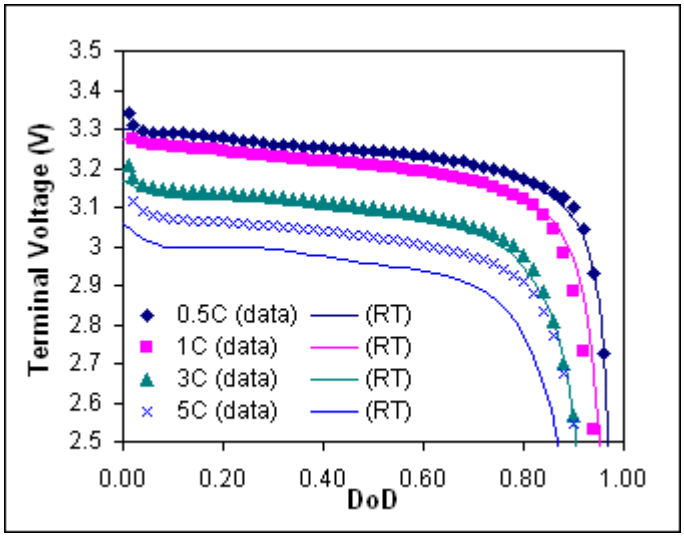

Figure 8. Terminal voltage predicted by RadTherm compared to measurements taken at 25 ºC.

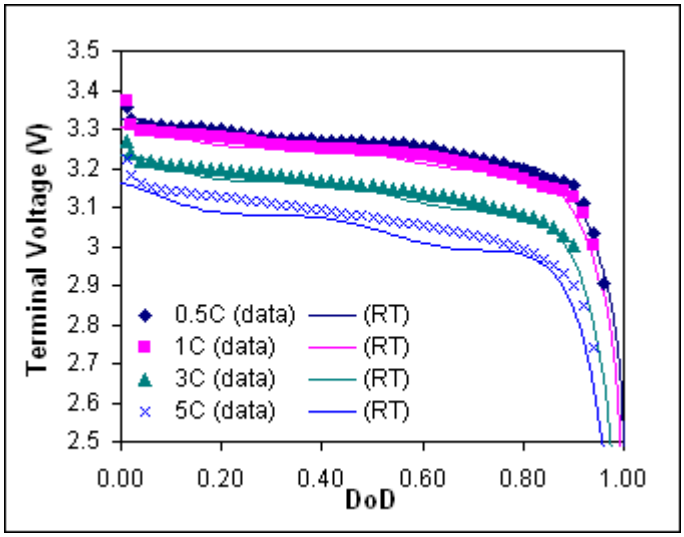

Figure 9. Terminal voltage predicted by RadTherm compared to measurements taken at 45 ºC.

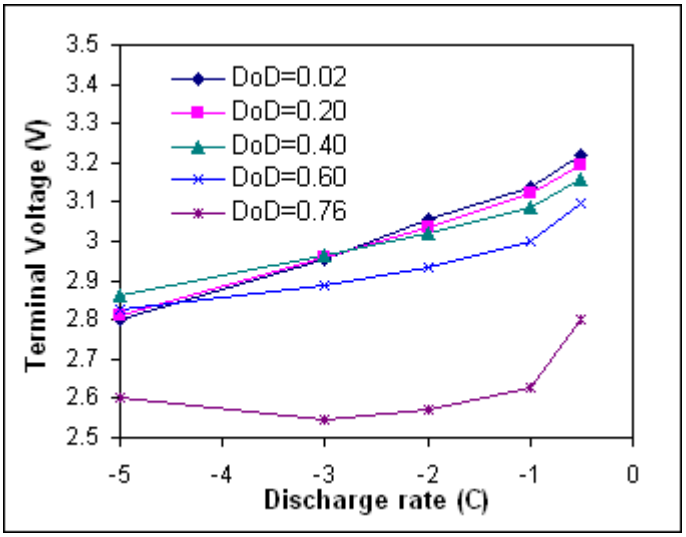

Figure 10. The measured current-voltage characteristic of the cell at 5 ºC is not linear.

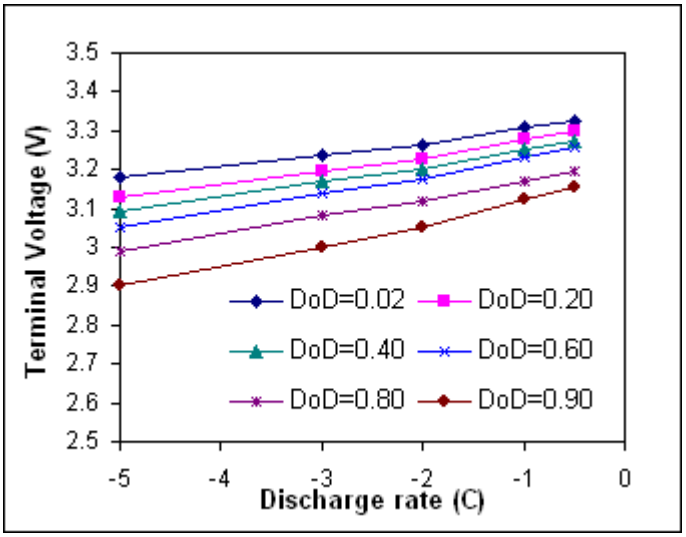

Figure 11. At 45 ºC the current-voltage characteristic fits the model assumption well.

Temperature comparisons are shown in Figures 12 to 14. Here the predicted values follow expected trends. The model tends to slightly underpredict temperature rise at low C rates, and overpredict the rise at higher discharge rates. The model temperature response depends on the heat generated by losses in the cell, the thermal mass of the cell, and the heat transfer to the environment. The inputs these factors depend on had to be estimated for this cell, as accurate input data was unavailable. Within the limits of the ability to estimate these input values, the agreement between measured and computed temperature seems quite reasonable. Access to more definitive information on the properties of the cell would lead to better agreement between model and measurement.

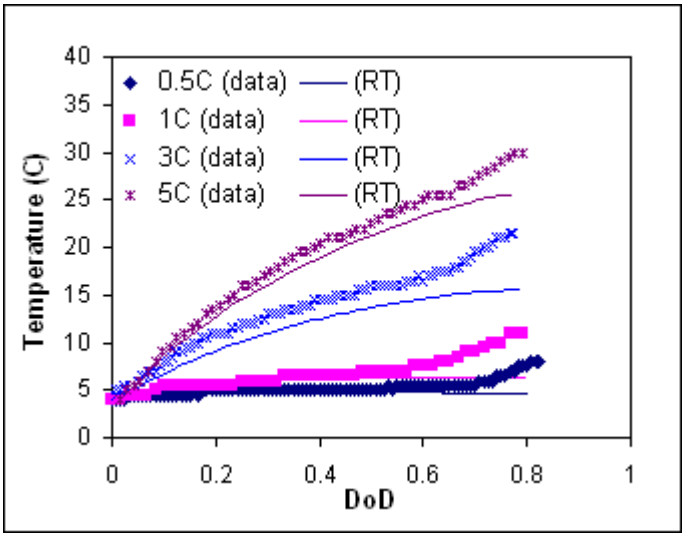

Figure 12. Temperature predictions compared to measured data at 5 ºC

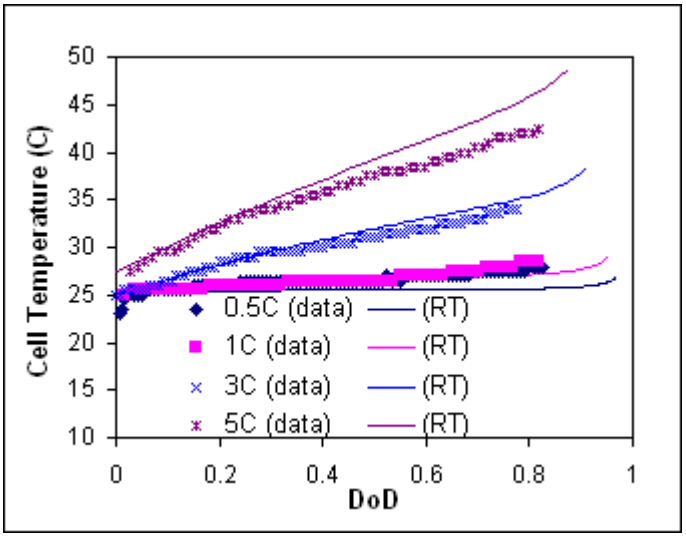

Figure 13. Temperature predictions compared to measured data at 25 ºC

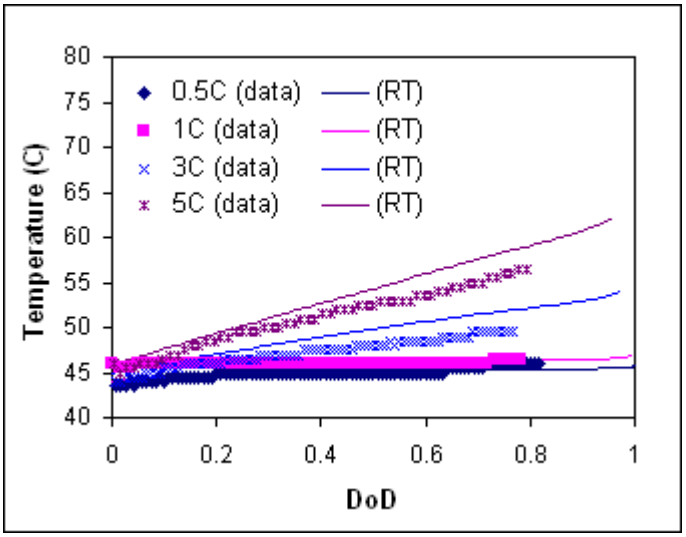

Figure 14. Temperature predictions compared to measured data at 45 ºC

MODELING STUDIES

The RadTherm model is suited to several types of battery studies. The flexibility of the model lies in the ability to apply different thermal and electrical boundary conditions to a cell or group of cells. Additional flexibility lies in the ability to use a fine mesh to focus on design details on a single cell, or a coarser mesh to look at pack cooling designs, or even modeling cells as single elements to form a pack model integrated into a full vehicle model. Examples of these types of studies are illustrated in the following paragraphs. It should be noted that the models are contrived, and the significance of the results is to demonstrate the capabilities of the approach.

CELL TAB LOCATION

The battery model combines an empirical current-voltage characteristic with a two-dimensional description of the voltage distributions on the anode and cathode collectors. Therefore it can be used to explore the effects of parameters that impact the voltage distribution. These types of studies can be performed in detail by applying the model to fine-mesh descriptions of single cells.

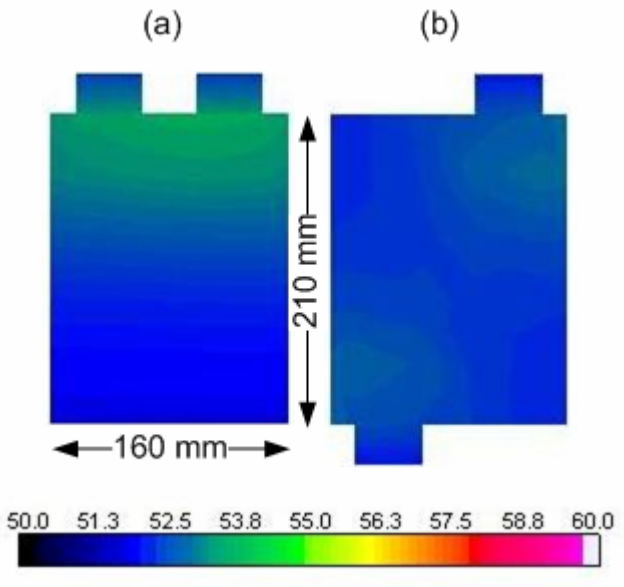

Figure 15. Cell temperatures at end of 5C discharge for two tab configurations.

For example, the model can capture the interplay between the lateral impedance of the collector plates and the vertical impedance of the electrodes that determines the distribution of current density over the area of the electrodes. Local regions of high current density produce thermal hot spots, but also lead to early charge depletion. The initial non-uniformity is a consequence of the position of the tabs, the aspect ratio of the cell, and the thickness of the collector plates. The resulting non-uniform temperature response is illustrated in Figure 15, for two different tab configurations. Temperatures at the end of a 5C discharge are shown. At the nominal aspect ratio (160:210), the difference in temperature is only about 1 °C. At a higher aspect ratio, the difference is exaggerated, as shown in Figure 16. Now the temperature difference is closer to 2°C. On the other hand, the effect of a higher aspect ratio can be mitigated with tab location. This can be seen by comparing the temperature contours of Figure 15(a) with those in Figure 16(b).

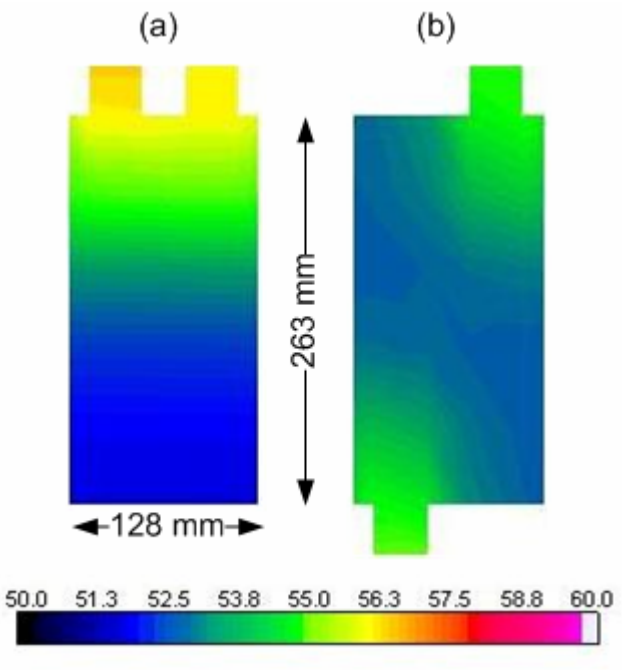

Figure 16. The model can quantify effect of cell aspect ratio on temperature at end of 5C discharge.

PACK COOLING STRATEGIES

The battery model can also be applied to multiple cells connected in series / parallel pack configurations. Here the focus of the analysis might be on the effectiveness of various cooling strategies, and the uniformity (in temperature and state of charge) from cell to cell. The mesh representing the thermal part of the RadTherm model integrates seamlessly with other RadTherm thermal modeling constructs. This makes it possible to add thermal boundary conditions representing a cooling strategy, and to perform parametric studies of the effect of selected cooling system parameters. For example, 3 cooling strategies are shown in Figure 17: no active cooling, a scheme where air is blown through the pack, and an approach where a plate in contact with one side of the cells in the pack is cooled along the bottom edge. In the no active cooling scheme, the cells are insulated on both sides. With active cooling, the cell temperatures are determined by convective cooling to a stream of air flowing through the cells. The stream is represented by a series of fluid nodes with advective links between them. In this case the effect of a mal-distribution of flow is investigated. Finally, conductive edge cooling to a cold plate is accomplished by modeling coolant flowing through a pipe attached to one edge of the cold plate.

The temperatures resulting from each cooling scheme (with two different flow rates for the air forced through the pack) are shown in Figure 18. The effect of flow rate on the forced air concept can be seen, and the efficiency of edge cooling to a cold plate versus direct forced air cooling can be compared.

To produce these temperature plots, the pack model was subjected to a power profile derived from a standard drive cycle[7]. The power profile was taken from a study done on a particular vehicle subjected to the INRETS URB1 drive cycle. The reader is referred to reference [7] for details.

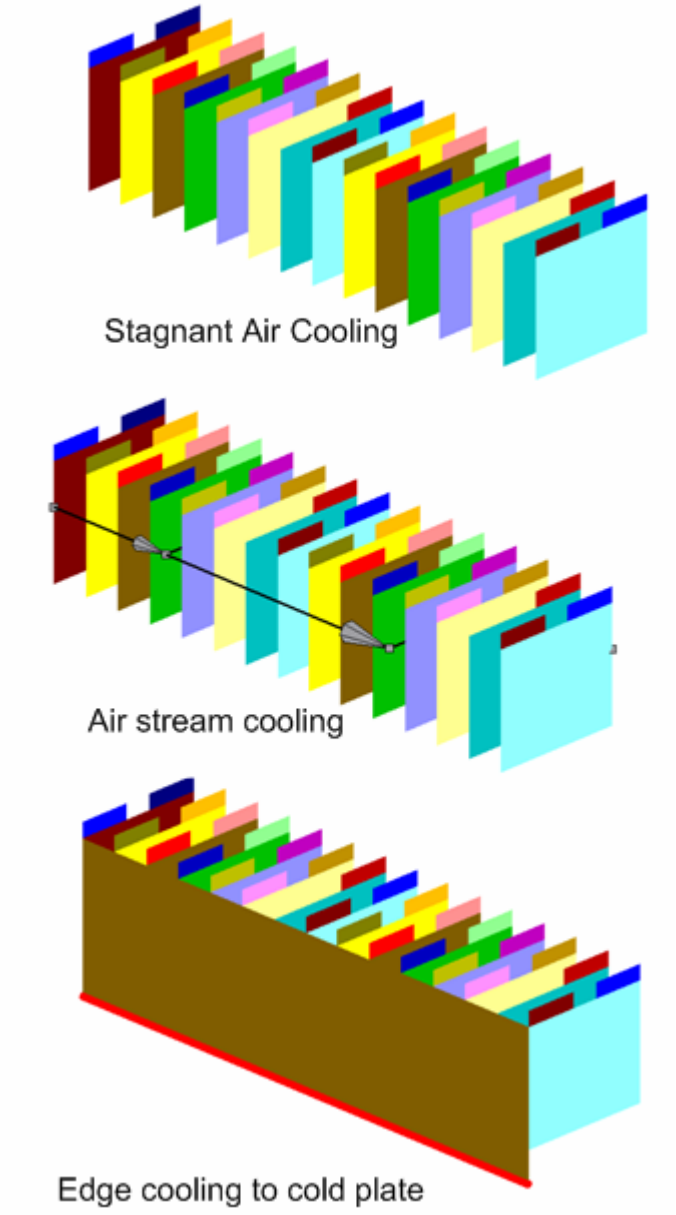

Figure 17. Three cooling options for a pack subjected to a typical drive cycle were investigated.

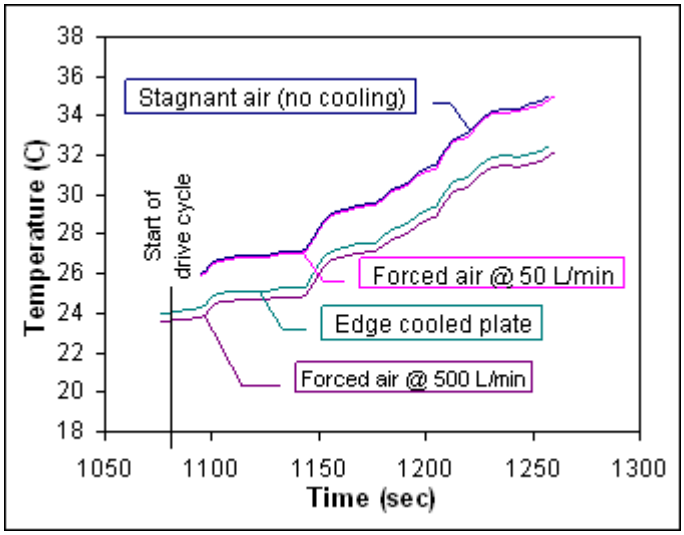

Figure 18. The temperature response at the center of a pack model for 4 different cooling options.

DRIVE CYCLE SIMULATION

The battery model can also be integrated into a full vehicle model to simulate the effect of the battery on the vehicle as well as the effect of the vehicle on the battery. Because the focus is not on the detailed response of individual cells, the mesh density can be greatly reduced for a pack-in-vehicle model. With fewer elements in the electrical part, the model behaves more like an equivalent circuit model, with the parameter U playing the part of an internal voltage source, and Y the part of an internal conductance. With a minimum element count, longer transients of a full vehicle become practical. It is straightforward, using the mechanisms available in RadTherm to impose heat on an element (tables, curves, or user routines), to assign a current load on a pack representing some drive cycle scenario. Figure 19 illustrates a battery pack and thermal management system incorporated into a full vehicle model. From models such as these, the thermal interaction between potentially critical vehicle components and a battery pack can be investigated. For example, the thermal environment resulting from imposition of a solar load, which perhaps might be modulated by a rear window, can be investigated. Other studies might investigate the integration of the pack thermal management system with the cabin HVAC system, or how best to warm up a battery in cold startup conditions.

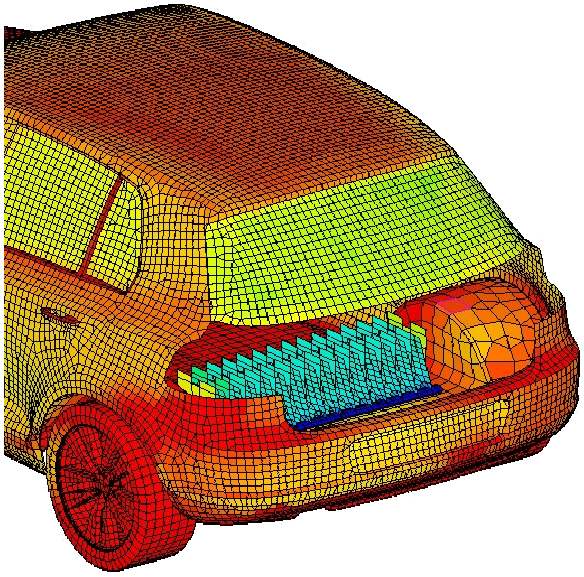

Figure 19. Example of a pack model integrated into a full vehicle model.

CONCLUSIONS

An empirical model of the current transfer between electrodes of a pouch type cell has been incorporated into the thermal analysis code RadTherm. The model predicts current density and voltage distribution on the electrodes of the cell, as well as local heating in the electrodes. The current transfer model is dependent on the local depth of discharge on the electrodes and the environmental temperature of the cell. These quantities are updated continuously during transient simulations.

The model predictions of terminal voltage and cell surface temperature have been shown to agree well with measurements from cells undergoing constant current discharges at rates from one half to five times the rated discharge current. The agreement occurs over environmental temperatures ranging from 0 °C to 45 °C.

The model has the flexibility to be useful for design studies of individual cells, of cell pack cooling systems, and of battery pack integration into vehicles. The implementation in RadTherm gives a user access to a variety of thermal boundary conditions at the cell, pack, and system levels. Transient current loads can be imposed, as well as transient thermal environments. Model outputs include the voltage distribution on the anode and cathode collector plates, the current density distribution over the electrodes, the total heat load on a cell, the temperature distribution on the electrodes, and the depth of discharge of a cell.

Future development of the model will focus on modifying the curve fit parameters to represent dependence on cell temperature rather than environmental temperature. This will allow more accurate modeling of the two-way coupling between the thermal and electrical behavior of a cell.

Disclaimer: Reference herein to any specific commercial company, product, process, or service by trade name, trademark, manufacturer, or otherwise, does not necessarily constitute or imply its endorsement, recommendation, or favoring by the United States Government or the Department of the Army (DoA). The opinions of the authors expressed herein do not necessarily state or reflect those of the United States Government or the DoA, and shall not be used for advertising or product endorsement purposes.

REFERENCES

1. Curran, A., RadTherm (Version 10.1), Computer Software, ThermoAnalytics Inc., Calumet, MI, 2011.
2. Kim, U.S., Shin, C.B., Kim, C., “Modeling for the Scale-up of a Lithium-Ion Polymer Battery,” *J. Power Sources*, **189**: 841-846, 2009.

3. Newman, J., Tiedemann, W., "Potential and Current Distribution in ElectroChemical Cells," *J. ElectroChem. Soc.* **140(7)**: 1961-1968, 1993.
4. Gu, H., "Mathematical Analysis of a Zn/NiOOH Cell," *J. ElectroChem. Soc.* **130**(7): 1459-1464, 1983.
5. Srinivasan, V., Wang, C.Y., "Analysis of Electrochemical and Thermal Behavior of Li-Ion Cells," *J. ElectroChem. Soc*. **150(1)**: A98-A106, 2003.
6. Gerver, R.A., "3D Thermal-Electrochemical Lithium-Ion Battery Computatiuonal Modeling,", Master's Thesis, University of Texas at Austin, 2009.
7. Duvall, M., "Battery Evaluation for Plug-In Hybrid Electric Vehicles," Vehicle Power and Propulsion 2005 IEEE Conference, September 2005.

CONTACT INFORMATION

Scott D. Peck

(906)-482-9560 x208

sdp@thermoanalytics.com

ACKNOWLEDGMENTS

The authors wish to thank A123 Systems for supplying the cells that were tested, and for providing additional data supporting the validation of the model. Also providing invaluable assistance was Elise Libby of TARDEC, who ran the tests and made the measurements, and Aaron Ditty of ThermoAnalytics, who supported the test set-up and data collection.